ELSEVIER

Journal of Power Sources 72 (1998) 1–8

JOURNAL OF POWER SOURCES

Electrochemical performance and chemical properties of oxidic cathode materials for 4 V rechargeable Li-ion batteries

A. Ott [a], P. Endres [a], V. Klein [a], B. Fuchs [a], A. Jäger [a], H.A. Mayer [a], S. Kemmler-Sack [a,*], H.-W. Praas [b], K. Brandt [b], G. Filoti [c], V. Kunczer [c], M. Rosenberg [d]

[a] *Institut für Anorganische Chemie, Auf der Morgenstelle 18, 72076 Tübingen, Germany*
[b] *VARTA Batterie AG, Gundelhardtstr. 72, 65779 Kelkheim, Germany*
[c] *Institute of Physics and Technology of Materials, 76900 Bucharest, Romania*
[d] *Ruhr-Universität Bochum NB03 / 32, 44780 Bochum, Germany*

Received 28 July 1997; accepted 14 October 1997

Abstract

The systems $Li_{1+x}Mn_{2-x}O_{4-\delta}$ and $Li_{1-x}Ni_{1+x}O_2$ were studied as oxidic cathode materials for 4 V rechargeable Li-ion cells. From a comparison of the results it follows that the spinel system can be subdivided into three regions: in region I ($0 \leq x < 0.05$) the electrochemical performance is unsatisfying due to a large volume reduction of about 7.5%, inducing stress, multiphase materials and capacity fading. Region II ($0.05 \lesssim x \lesssim 0.2$) contains the best cathode material with a composition near $x = 0.1$. The spinel framework is stable against Li extraction. In region III ($0.2 \leq x \leq 1/3$) the capacity is too low for an application in the 4 V region. In the system $Li_{1-x}Ni_{1+x}O_2$ the highest capacity is observed for $LiNiO_2$ with $x = 0$. Experimental difficulties during material synthesis were overcome by suppression of the decomposition of $LiNiO_2$ into $Li_{1-x}Ni_{1+x}O_2$, Li_2O and O_2.

Keywords: Li-ion cells; Oxidic materials; Rechargeable batteries; 4V material

1. Introduction

Oxidic materials which can be used as cathodes in 4 V rechargeable Li cells are the layered oxides $LiCoO_2$ and $LiNiO_2$ of α-$NaFeO_2$ type (space group $R\bar{3}m$ [1]) and the cubic spinel $LiMn_2O_4$ ($Fd\bar{3}m$ [2–6]). $LiNiO_2$ is the Li rich endmember of the system $Li_{1-x}Ni_{1+x}O_2$ and difficult to prepare [7,8]. Solid solutions of $LiNi_{1-x}Co_xO_2$ have also been investigated as electrodes in such cells [9]. For $x = 0.5$ the compound is easier to obtain than $LiNiO_2$ but has almost the same voltage profile. The voltage of $Li/LiNiO_2$ cells is about 0.25 V lower than $Li/LiCoO_2$ cells making the former less prone to electrolyte oxidation problem to high temperatures [10]. In addition, Ni is less expensive than Co and is more abundant, so $LiNiO_2$ and its Ni rich solid solutions may be more useful than $LiCoO_2$. From the point of view of starting material, price and toxicity, the $LiMn_2O_4$ spinel has a considerable advantage. However, its rechargeable capacity and cyclability in the 4 V region are inferior to that of the layered oxides. Several attempts to improve the electrochemical performance have been reported. The most effective candidate is low valent cation doping to 16d sites (denoted in square brackets), $Li[M_xM_{2-x}]O_4$ [11]. Monovalent Li doping seems to be the best since a small fraction of dopant is effective (due to the large charge difference relative to Mn) and lattice disturbances are minimized. A second advantage of Li doping is the prevention of foreign ions from occupying tetrahedral 8a sites which will hamper the migration of Li between the 8a and 16c sites, resulting in a decrease of rechargeable capacity. Investigations of the recently synthesized Li-rich spinels of type $Li[Li_xMn_{2-x}]O_4$ [4,12] reveal a slight oxygen deficiency: $Li_{1+x}Mn_{2-x}O_{4-\delta}$ [5,6,13]. Furthermore, the rechargeable capacity is strongly dependent on the Li/Mn ratio [4,6,13].

To get a better insight into the electrochemical performance the aim of the present investigation was to study the influence of the Li content on the electrochemical, chemical and magnetic properties of several members of the spinel phase $Li_{1+x}Mn_{2-x}O_{4-\delta}$ and the ordered rocksalt α-$NaFeO_2$ type of the Li-rich phase $Li_{1-x}Ni_{1+x}O_2$.

* Corresponding author. Fax: +49-0-7071-296918.

0378-7753/98/$19.00

2. Experimental

For the synthesis of the series $Li_{1+x}Mn_{2-x}O_{4-\delta}$ the starting materials β-MnO_2 (Selectipur, Merck) and $LiOH \cdot H_2O$ (Alfa Ventron) were thoroughly mixed in an agate mortar and heated in corundum boats (Degussit Al 23) in air between 400 and 850°C for 4 h and 16 h with an intermittent regrinding and X-ray analysis (XRD, Philips powder diffractometer, Ni-filtered CuKα radiation, Au standard). All materials were quenched to room temperature. The correlation between the reaction temperature and the parameter x as well as the experimental conditions for Li extraction with Br_2/CH_3CN and H_2SO_4/H_2O are indicated in Ref. [13].

For the synthesis of Li-rich members of the system $Li_{1-x}Ni_{1+x}O_2$ the thoroughly ground starting materials Li_2O_2 (Alfa Ventron corrected for a content of 5% Li_2CO_3) and NiO (Johnson Matthey) were pelletized. Two pellets were put one on top of the other in an alumina container and fired in flowing oxygen for 48 h at 700°C with three intermittent regrindings. The upper pellet was employed for the further investigations.

Susceptibility and Mössbauer spectroscopic measurement were performed according to Ref. [14]. NMR spectra were recorded as in Ref. [13].

3. Results and discussion

3.1. System $Li_{1+x}Mn_{2-x}O_{4-\delta}$

3.1.1. XRD and electrochemical performance

In the series $Li_{1+x}Mn_{2-x}O_{4-\delta}$ a complete series of solid solutions is existing for $0 \leq x \leq 0.33$. All materials crystallize in the cubic spinel structure of space group $Fd\bar{3}m$. The oxygen deficiency increases with increasing x.

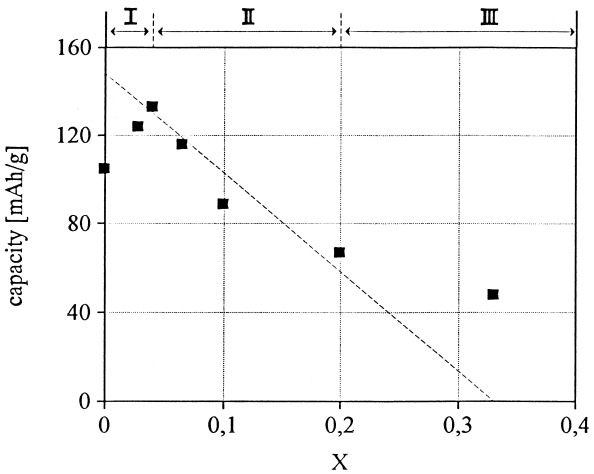

Fig. 1. The first charge capacity (3.3–4.3 V) of the spinel phase $Li_{1+x}Mn_{2-x}O_{4-\delta}$. The broken line is the theoretical capacity for $\delta = 0$.

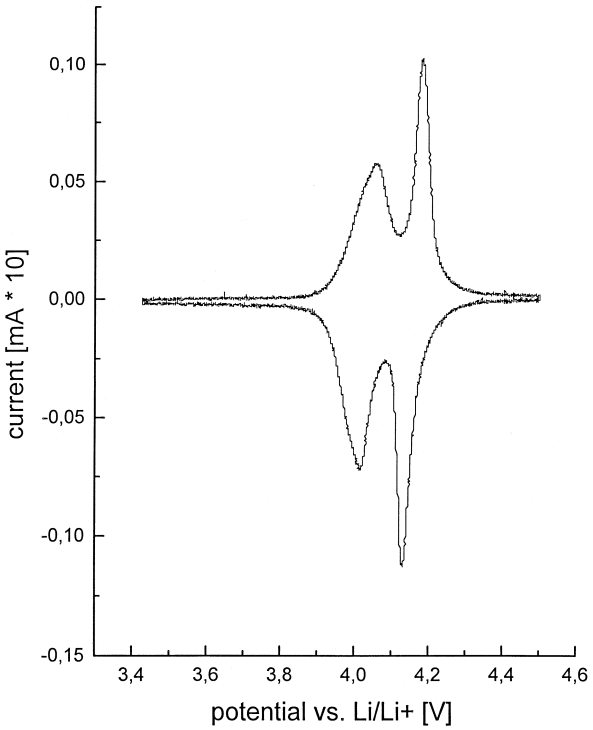

Fig. 2. Cyclic voltammogram of $LiMn_2O_4$.

The lattice constants vary linearly between 8.247 Å ($x = 0$, $\delta = 0$) and 8.157 Å ($x = 0.33$, $\delta = 0.13$ [13]).

The electrochemical Li extraction from the system $Li_{1+x}Mn_{2-x}O_{4-\delta}$ is accompanied by an oxidation of Mn^{3+} to Mn^{4+}. The theoretical capacity for the case of $\delta = 0$ is indicated in Fig. 1 together with values of the first charge capacity (3.3–4.3 V). The electrochemical performance can be roughly divided in three regions: in region I ($x \lesssim 0.05$) the experimental capacity is inferior to the theoretical value, in region II ($0.05 \lesssim x \lesssim 0.2$) both values are in fairly good agreement whereas in region III ($0.2 \lesssim x \leq 0.33$) the electrochemical performance is better than expected for the case of $\delta = 0$.

Li/Mn-spinels are three-dimensional Li-ion conductors. Li^+ extraction from $LiMn_2O_4$ is accompanied by a high volume reduction of 7.5% between the starting material and the fully extracted spinel. This large volume decrease is considered as one reason for the pronounced fading of the rechargeable capacity [6,15,16]. Li^+ ions are inserted and extracted into the spinel phase by a two-step process; illustrated by two pairs of redox peaks in the cyclic voltammogram of Fig. 2. From the crystallographic point of view this behaviour is explained by the splitting of the original Li positions in 8a with the coordinates 0, 0, 0; 1/4, 1/4, 1/4, (space group $Fd\bar{3}m$) in two sets of sites: 4a (0, 0, 0) and 4c (1/4, 1/4, 1/4); space group $F23$. Firstly, Li is removed from half of the tetrahedral positions with strong Li–Li interaction (site 4a), affording less energy (oxidation potential at about 4.0 V vs. Li/Li^+) than for the second set (4c) with the higher potential of

about 4.15 V. Li extraction from 4c affords more energy due to the stronger attractive forces as a result of the increasing content of higher valent Mn^{4+}.

By application of Br_2/CH_3CN with a redox potential of Br_2/Br^- in CH_3CN vs. Li^+/Li of 4.1 V [17] as extraction medium for the system $Li_{1+x}Mn_{2-x}O_{4-\delta}$ we were able to remove only the first set of Li ions with a potential of about 4.0 V, whereas the deeper positions remain unaffected. Accordingly, the decrease of the unit cell volume is relatively small and situated between ≈ 3% for $x = 0.0$ (lattice constant of the extraction product: $a = 8.165$ Å, main phase) and ≈ 1% for $x = 0.33$ (8.157 Å [13]). The XRD diagrams of the extraction residues in Fig. 3 indicate that Li-rich spinel with $0.1 \leq x \leq 0.33$ yield single phase material with the typical diffraction pattern of a cubic spinel. However, for $x = 0$ and 0.05 multiphase material is formed, easily visible from the appearance of several satellite peaks in the XRD. By acidic Li extraction with e.g., H_2SO_4/H_2O both Li positions are accessible. However, even deep acidic Li extraction results uniformly in multiphase samples [6,13]. It is very likely that the tendency of Li ordering is responsible for this effect. Due to the fact that certain Li:□ ratios on the tetrahedral position will be more suitable for cationic ordering than others several ordered phases of different stability are simultaneously produced.

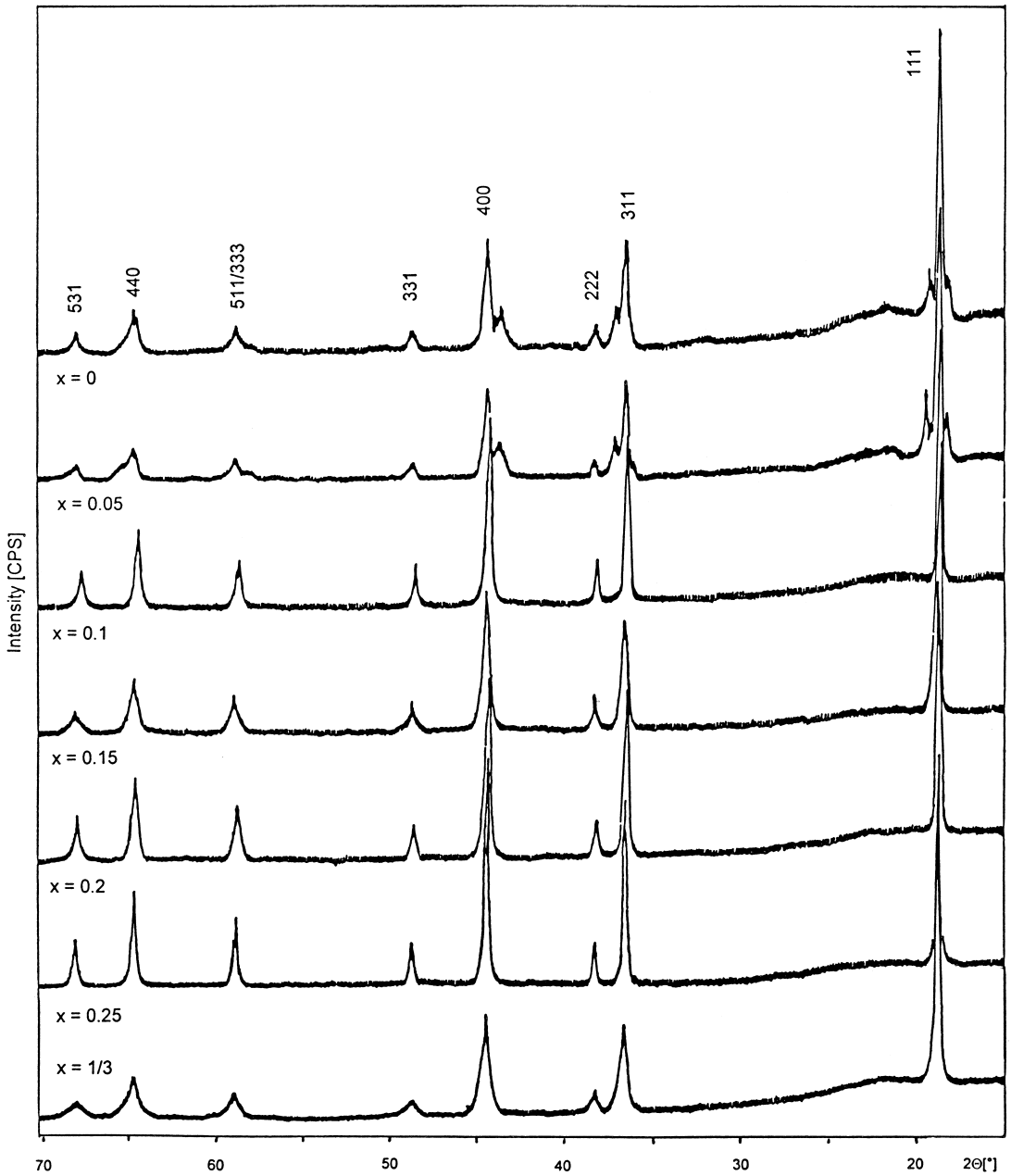

Fig. 3. XRD diagrams of residues for Br_2/CH_3CN extraction of Li from the spinel system $Li_{1+x}Mn_{2-x}O_{4-\delta}$. The Miller indices are given for each Bragg peak with reference to the setting of the cubic spinel cell ($Fd\bar{3}m$). For clarity the spectra are shifted along the y axis.

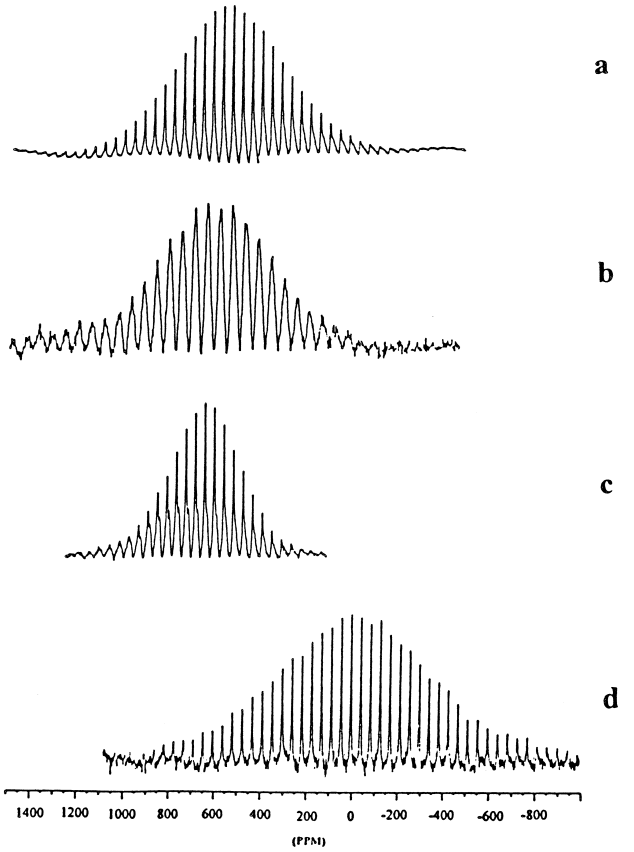

Fig. 4. {^{7}Li} MAS-NMR spectra of (a) $LiMn_2O_4$ ($x = 0$), (b) $Li_{1.2}Mn_{1.8}O_{3.93}$ ($x = 0.2$), (c) $Li_{0.6}Mn_2O_4$ (Br_2/CH_3CN extraction) and (d) $LiCrMnO_4$.

3.1.2. {^{7}Li} MAS-NMR spectra

The ^{7}Li NMR spectra of some members of the system $Li_{1+x}Mn_{2-x}O_{4-\delta}$ and its extraction products are shown in Fig. 4 together with the spectrum of $LiCrMnO_4$. For all compounds the NMR spectrum exhibits a single line spaced by spinning side bands. The Knight shift for the system $Li_{1+x}Mn_{2-x}O_{4-\delta}$ are uniformly situated around 550 ppm (cf. the spectra for $x = 0$ and 0.2 in Fig. 4a,b). Moreover, Li extraction does not influence the position of the ^{7}Li NMR signal of the remaining Li; situated for e.g., $Li_{0.6}Mn_2O_4$ and other extraction products invariably in the 550 ppm region (Fig. 4c). The quantity of the Knight shift of $LiMn_2O_4$ is in agreement with the data from the literature [18,19]. The calculated electron density of ≈ 0.9 (electron density of Li in the compound/electron density of Li in atomic state) is higher than for Li metal (0.44 [20]). This means that an average of 90% of 2s electrons is located at the lithium nucleus and Li exists in an almost atomic state.

For comparison we synthesized the well known spinel $LiCrMnO_4$ with the fixed cationic valences Cr^{3+} and Mn^{4+} [21,22]. This compound does not show any Knight shift and lithium exists in completely ionic state with an apparent valency of $+1.0$. Interestingly, this spinel is not accessible for a Li extraction with Br_2/CH_3CN.

3.1.3. Magnetic susceptibility and Mössbauer spectroscopy

The temperature dependence of the magnetic susceptibility of spinels of the system $Li_{1+x}Mn_{2-x}O_{4-\delta}$ indicate

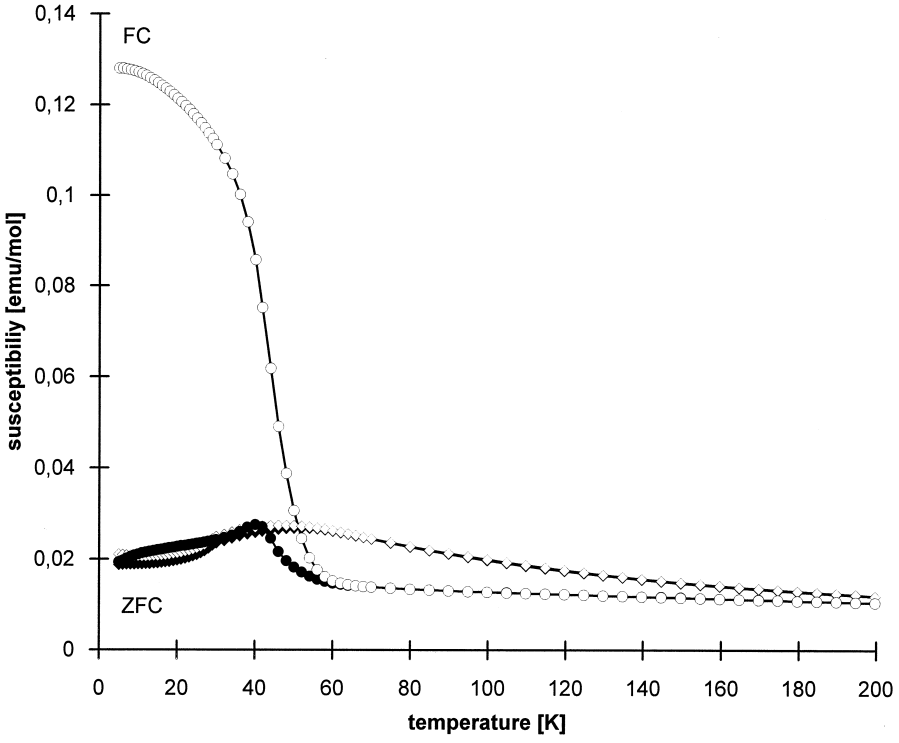

Fig. 5. χ vs. T for ^{57}Fe doped (○) $LiMn_2O_4$ and (◇) $Li_{0.15}Mn_2O_4$; FC: field cooled, ZFC: zero field cooled; $B = 0.1$ T.

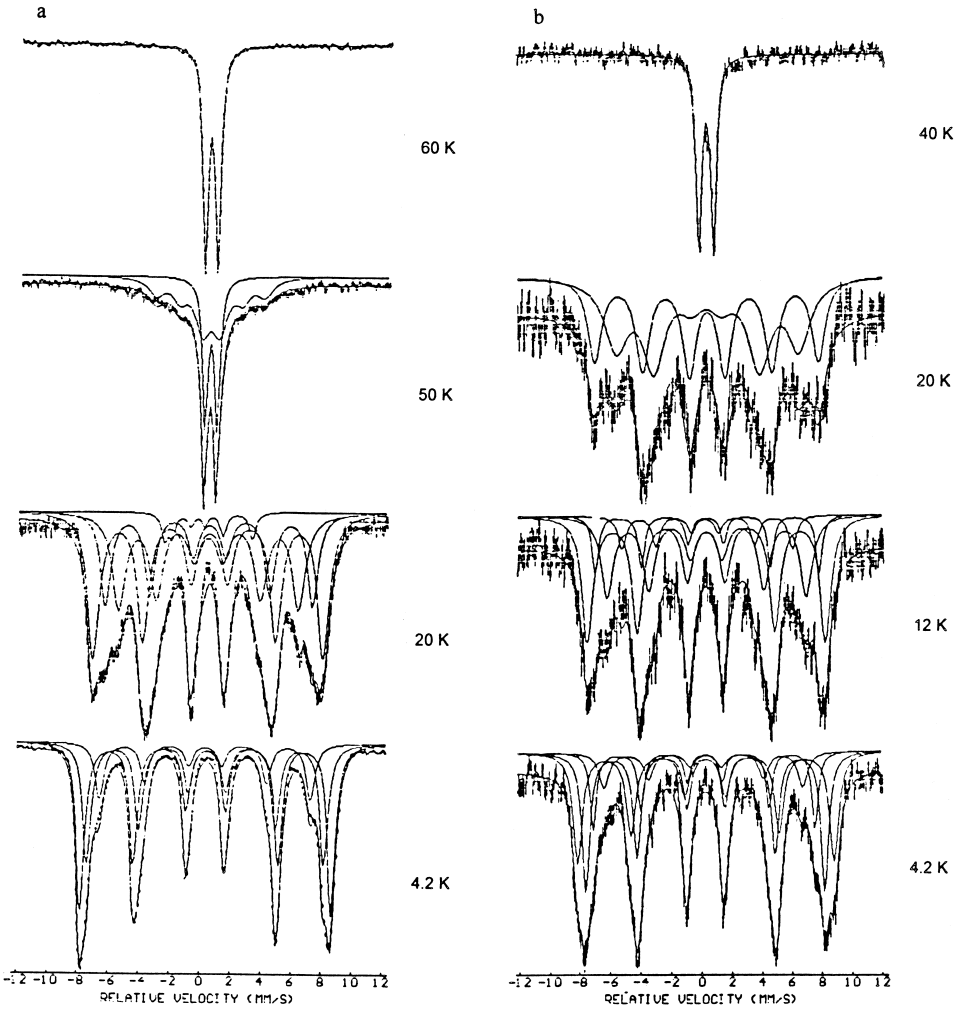

Fig. 6. Mössbauer spectra of ^{57}Fe doped (a) $LiMn_2O_4$ and (b) $Li_{0.15}Mn_2O_4$ taken at several temperatures.

the validity of the Curie–Weiss law at higher temperatures. Below a freezing temperature T_F a spin glass behaviour develops. T_F decreases with increasing x from around 55 K ($x = 0$) to about 10 K ($x = 0.33$ [5]). In the delithiated material the reduction of the Mn^{3+} content reduces the total magnetical susceptibility and induces a practically antiferromagnetic behaviour below about 50 K. Fig. 5 indicates the χ vs. T traces for $LiMn_2O_4$ and $Li_{0.15}Mn_2O_4$.

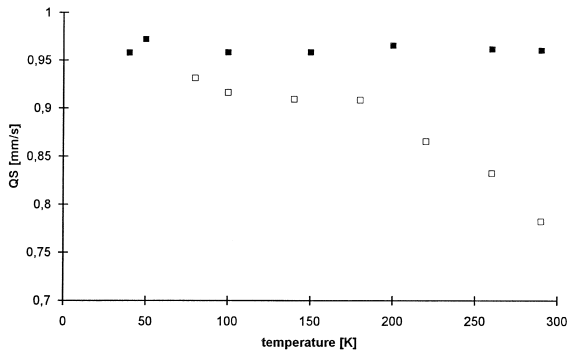

Fig. 7. Temperature dependence of the quadruple splitting for (□) $LiMn_2O_4$ and (■) $Li_{0.15}Mn_2O_4$.

From the Mössbauer spectra of ^{57}Fe doped $LiMn_2O_4$ and $Li_{0.15}Mn_2O_4$ in Fig. 6 it follows the existence of a low temperature state with frozen and possibly ordered spins in a kind of antiferromagnetic configuration. A good fit of the 4.2 K spectra needed either a distribution of hyperfine fields or four different Lorenzian sextets with hyperfine fields between 52 and 43 T. The hyperfine fields decrease with increasing temperature but for some Fe spins a relaxation occurs which gives rise to a strong intensive Mössbauer doublet in the central part well below the critical temperature.

A very interesting finding is a Mössbauer spectroscopic evidence for the Jahn–Teller effect in $LiMn_2O_4$. Its content of 50% of Mn^{3+} in octahedral positions is very close to the critical concentration for the occurrence of the Jahn–Teller distortion. As was shown previously [23] the

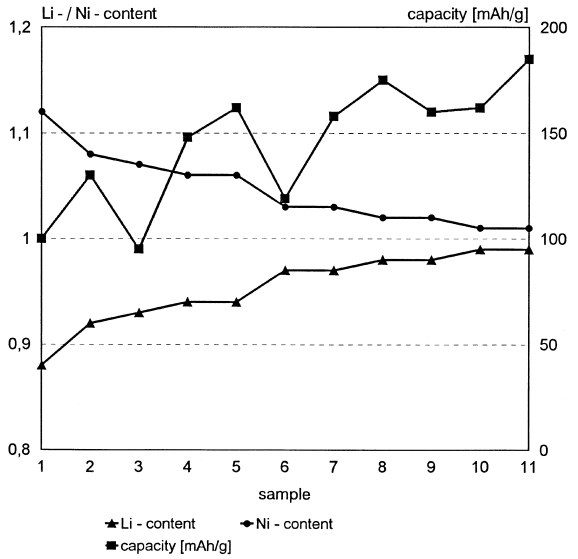

Fig. 8. Rechargeable capacity vs. Li/Ni content for several materials of the system $Li_{1-x}Ni_{1+x}O_2$.

quadrupole splitting (QS) of Fe ions in the Mn surroundings of the spinels $CdMn_2O_4$ and $ZnMn_2O_4$ is a measure for the local Jahn–Teller distortion around the Fe ion. As one can see from Fig. 7 the QS of $LiMn_2O_4$ starts to decrease rapidly above 200 K due to a transition from the Jahn–Teller distorted to a non-distorted cubic structure. In contrast the QS of $Li_{0.15}Mn_2O_4$, where one has a very low Mn^{3+} content of 15%, is practically independent of temperature, indicating the absence of any Jahn–Teller effect.

Table 1
Average oxidation state of Ni (Ox(Ni)), Li/Ni ratio and resoluting composition for some Li-rich materials of the system $Li_{1-x}Ni_{1+x}O_2$

Ox(Ni)	Li/Ni ratio	Composition
+2.86	0.88	$Li_{0.94}Ni_{1.06}O_2$
+2.95	0.94	$Li_{0.97}Ni_{1.03}O_2$
+3.00	1.00	$Li_{1.00}Ni_{1.00}O_2$

Our results are in good agreement with the data of Yamada and Tanaka [24], who found evidence for a Jahn–Teller distortion for $LiMn_2O_4$ around 280 K from thermal analysis and XRD. The observed tremendous increase up to 60% between 280 and 260 K with about 65% of the distorted tetragonal phase at 220 K, what we also see in the ^{57}Fe QS.

3.2. System $Li_{1-x}Ni_{1+x}O_2$

3.2.1. XRD and electrochemical performance

Several Li-rich members of the system $Li_{1-x}Ni_{1+x}O_2$ with $0.0 \leq x \lesssim 0.1$ were studied. They can be prepared as single phase materials if the decomposition into Li_2O, oxygen and a Ni-rich phase is suppressed. For $LiNiO_2$ the following relation is valid:

$$2LiNi^{3+}O_2 \rightarrow Li_{1-x}Ni^{3+}_{1-x}Ni^{2+}_{2x}O_2 + xLi_2O + x/2O_2$$

All prepared Li-rich materials crystallize in the α-$NaFeO_2$ type of space group $R\bar{3}m$. In this Li-rich region the lattice constants are very similar and not indicative for

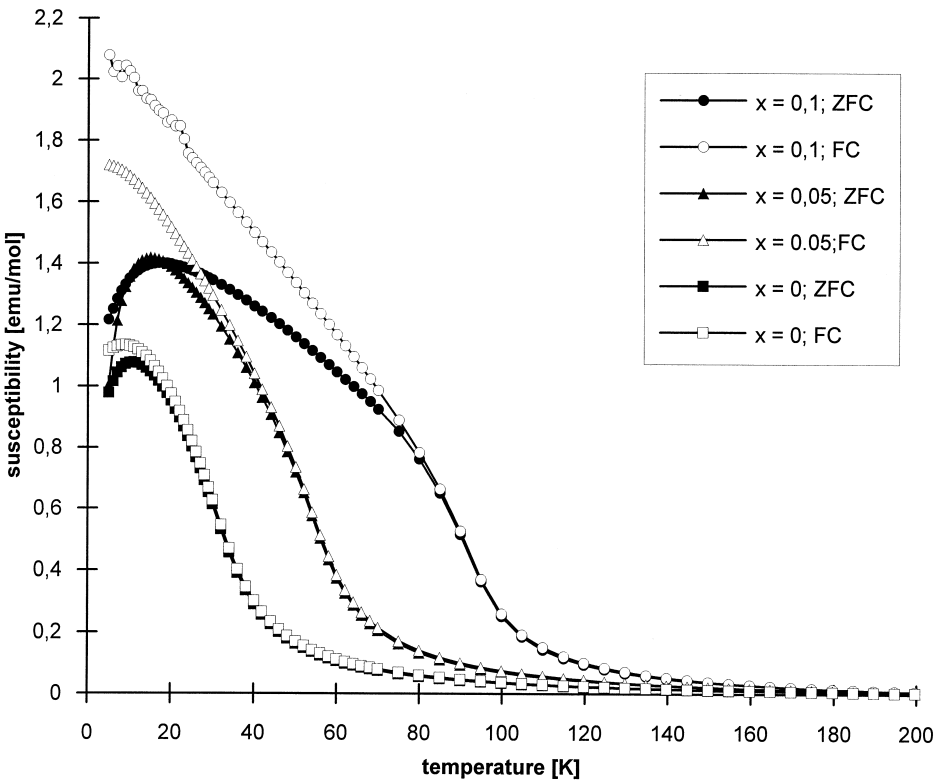

Fig. 9. χ vs. T for some Li-rich members of the system $Li_{1-x}Ni_{1+x}O_2$; FC: field cooled, ZFC: zero field cooled; $B = 0.1\ T$.

the individual composition (e.g., $x = 0.08$: $a = 2.885$; $c = 14.21$ Å; $x = 0.01$: $a = 2.884$, $c = 14.21$ Å (hexagonal setting)). However, the electrochemical performance strongly depends on the Li/Ni ratio since an excess of Ni enters into the Li layers with the result of a blockage of the two-dimensional Li migration paths. In agreement with several observations of other authors (e.g., [25,26]) the rechargeable capacity increases with increasing Li/Ni ratio (Fig. 8). The best values are observed for x around 0.0.

Due to the fact that the $x = 0.0$ compound $LiNiO_2$ contains a maximal Ni^{3+} content the determination of the average oxidation state of Ni by redox titration is a very reliable proof for the composition of the synthesized material. Table 1 gives some values together with the Li/Ni ratio (from AAS analysis) and the resulting composition.

3.2.2. Magnetic susceptibility

In the ideal rhombohedral structure of $LiNiO_2$ ($R\bar{3}m$, Li in 3a, Ni in 3b, O in 6c) the NiO_6 octahedra share edges to form a triangular Ni lattice. Nonmagnetic Li layers alternate with magnetic Ni layers, making the interlayer distance (4.73 Å) much longer than the intralayer distance (2.88 Å). So magnetic correlations between Ni ions are considered as two dimensional [27] and a frustrated antiferromagnetic $S = 1/2$ triangular lattice [28] or spin glass [29] may be anticipated. For $x > 0$ the excess of Ni occupies the Li positions 3a; thus creating a three dimensional connection between the two dimensional Ni layers (in 3b). Accordingly, the magnetic properties are strongly influenced by the Ni amount in site 3a. Moreover, the two-dimensionality of the magnetic interaction may be destroyed by a certain degree of disorder between Li in 3a and Ni in 3b. Again a three-dimensional magnetic correlation is introduced.

From the temperature dependence of the magnetic susceptibility of some Li-rich members of the system $Li_{1-x}Ni_{1+x}O_2$ in Fig. 9 it follows that the extend of the magnetic interactions increase with increasing x. An analysis of the magnetic properties reveal strong ferromagnetic correlations and spin freezing at low temperatures, reminding many characteristic features of spin-glass behaviour. The freezing temperature increases with increasing Ni content in 3a from 30 K for $x \approx 0.0$ via 54 K ($x = 0.05$) to 90 K for $x = 0.10$.

4. Conclusions

The electrochemical performance in the 4 V region of the spinel system $Li_{1+x}Mn_{2-x}O_{4-\delta}$ and of the ordered rocksalt phase $Li_{1-x}Ni_{1+x}O_2$ is strongly influenced by the parameter x. According to our studies of various chemical and physical properties the spinel system $Li_{1+x}Mn_{2-x}O_{4-\delta}$ can be subdivided into three regions:

In region I ($0 \leq x < 0.05$) the spinel framework is not stable against Li extraction. The electrochemical performance is unsatisfying due to the large volume reduction of about 7.5% between the starting material and the fully extracted spinel, including stress and capacity fading. The extraction products are always multiphase. Region II ($0.05 \lesssim x \lesssim 0.2$) contains the best cathode materials. The optimal composition is situated near $x = 0.1$. The spinel framework is stable against Li extraction. At different extraction levels always single phase materials are present. The volume drop decreases to about 5.5% ($x = 0.1$) and 4.5% ($x = 0.2$). All materials are slightly oxygen deficient. In region III ($0.2 \lesssim x \leq 0.33$) the host matrix is again stable against Li extraction. Due to an oxygen deficiency even spinels with $x = 0.33$ conserve a minor ability for Li extraction. However, the observed capacity is too low for an application in the 4 V region.

In the system $Li_{1-x}Ni_{1+x}O_2$ of α-$NaFeO_2$ type the highest capacity is observed for the ideal composition $LiNiO_2$ ($x = 0$). Due to the absence of Ni in the Li sheets the Li ions are not hampered from their two-dimensional migration. Experimental difficulties during material synthesis were overcome by suppressing the decomposition reaction $2\,LiNiO_2 \rightarrow Li_{1-x}Ni_{1+x}O_2 + Li_2O + x/2O_2$.

Acknowledgements

This work was supported by the Bundesministerium für Bildung, Wissenschaft, Forschung und Technologie as well as by the Verband der Chemischen Industrie.

References

[1] K. Mizushima, P.C. Jones, P.J. Wiseman, J.B. Goodenough, Mater. Res. Bull. 15 (1980) 783.
[2] M.M. Thackeray, W.I.F. David, P.G. Bruce, J.B. Goodenough, Mater. Res. Bull. 18 (1983) 461.
[3] M.M. Thackeray, P. Johnson, L.A. de Piciotto, P. Bruce, J.B. Goodenough, Mater. Res. Bull. 19 (1984) 179.
[4] R.J. Gummov, A. de Kock, M.M. Thackeray, J. Solid State Chem. 69 (1994) 59.
[5] P. Endres, B. Fuchs, S. Kemmler-Sack, K. Brandt, G. Faust-Becker, H.-W. Praas, J. Solid State Ionics 89 (1996) 221, and Refs. cited therein.
[6] S. Kemmler-Sack, B. Fuchs, P. Endres, H.-W. Praas, K. Brandt, GdCH-Monographie, in: F. Beck (Ed.), Vol. 3, Elektrochemie der Elektronenleiter, 1996, p. 342.
[7] R. Kanno, H. Kubo, Y. Kawamoto, T. Kaniyama, F. Izumi, Y. Takeda, M. Takano, J. Solid State Chem. 110 (1994) 219.
[8] A. Hirano, R. Kanno, Y. Kawamoto, Y. Takeda, K. Yamaura, M. Takano, K. Okyama, M. Ohashi, Y. Yamaguchi, Solid State Ionics 78 (1995) 123.
[9] T. Ohzuku, H. Komori, K. Sawai, T. Hirai, Chem. Express 5 (1990) 733.
[10] S.A. Campbell, C. Bowes, R.S. McMillan, J. Electroanal. Chem. 284 (1990) 195.
[11] A. Yamada, J. Solid State Chem. 122 (1996) 160.
[12] B. Fuchs, Diplomarbeit, Universität of Tübingen, 1990.
[13] P. Endres, A. Ott, S. Kemmler-Sack, A. Jäger, H.A. Mayer, H.-W. Praas, K. Brandt, J. Power Sources 69 (1997) 149.

[14] B. Seling, C. Schinzer, A. Ehmann, S. Kemmler-Sack, G. Filoti, M. Rosenberg, J. Linhart, W. Reimers, Physica C251 (1995) 238.
[15] T. Ohzuku, M. Kitagawa, T. Hirai, J. Electrochem. Soc. 137 (1990) 769.
[16] Y. Xia, M. Yoshio, J. Electrochem. Soc. 143 (1996) 825.
[17] A.R. Wizansky, P.E. Rauch, F.J. Disalvo, J. Solid State Chem. 81 (1989) 203.
[18] N. Kumagai, T. Fujiwara, K. Tanno, T. Horiba, J. Electrochem. Soc. 143 (1996) 1007, and Refs. cited therein.
[19] Y. Kanazaki, A. Tamiguchi, M. Abe, J. Electrochem. Soc. 138 (1991) 333.
[20] C. Ryter, Phys. Rev. Lett. 5 (1960) 10.
[21] A. Ott, Diplomarbeit, University of Tübingen, 1996.
[22] G. Blasse, J. Inorg. Nucl. Chem. 25 (1963) 743.
[23] G. Filoti, A. Geiberg, V. Gomolea, M. Rosenberg, Int. J. Magn. 2 (1972) 65.
[24] A. Yamada, M. Tanaka, Mater. Res. Bull. 30 (1995) 715.
[25] H. Arai, S. Okada, H. Ohtsuka, M. Ichimura, J. Yamaki, Solid State Ionics 80 (1995) 261.
[26] V. Klein, Dissertation, Universität of Tübingen, 1995.
[27] K. Yamaura, M. Takano, A. Hirano, R. Kanno, J. Solid State Chem. 127 (1996) 109, and Refs. therein.
[28] K. Hirakawa, H. Kadwaki, K. Ubrekoshi, J. Phys. Soc. Jpn. 54 (1985) 3526.
[29] M. Rosenberg, P. Stelmaszyk, V. Klein, S. Kemmler-Sack, G. Filoti, J. Appl. Phys. 75 (1994) 6813.